

## FAT-SPECIFIC PROTEIN 27 REGULATES STORAGE OF TRIACYLGLYCEROL

Pernille Keller<sup>\*1</sup>, John T. Petrie<sup>\*1</sup>, Paul De Rose<sup>1</sup>, Isabelle Gerin<sup>1</sup>, Wendy S. Wright<sup>1</sup>, Shian-Huey Chiang<sup>2</sup>, Anders R. Nielsen<sup>3</sup>, Christian P. Fischer<sup>3</sup>, Bente K. Pedersen<sup>3</sup>, and Ormond A. MacDougald<sup>1</sup>

<sup>1</sup>Department of Molecular & Integrative Physiology and <sup>2</sup>Life Sciences Institute, University of Michigan, Ann Arbor, Michigan 48109

<sup>3</sup>Centre for Inflammation and Metabolism, Rigshospitalet, University of Copenhagen, Denmark  
Address correspondence to: Ormond A. MacDougald, 7620 Med Sci II, 1301 E. Catherine St. Ann Arbor, MI 48109-0622, USA. Email: [macdougald@umich.edu](mailto:macdougald@umich.edu)

Running header: FSP27 in triacylglycerol storage

Fat-specific protein 27 (FSP27) is a member of the CIDE family. While *Cidea* and *Cideb* were initially characterized as activators of apoptosis, recent studies have demonstrated important metabolic roles for these proteins. In this study, we investigated the function of another member of this family, FSP27 (*Cidec*), in apoptosis and adipocyte metabolism. While overexpression of FSP27 is sufficient to increase apoptosis of 293T and 3T3-L1 cells, more physiological levels of expression stimulate spontaneous lipid accumulation in several cell types without induction of adipocyte genes. Increased triacylglycerol is likely due to decreased  $\beta$ -oxidation of non-esterified fatty acids. Altered flux of fatty acids into triacylglycerol may be a direct effect of FSP27 function, which is localized to lipid droplets in 293T cells and 3T3-L1 adipocytes. Stable knockdown of FSP27 during adipogenesis of 3T3-L1 cells substantially decreases lipid droplet size, increases mitochondrial and lipid droplet number, and modestly increases glucose uptake and lipolysis. Expression of FSP27 in subcutaneous adipose tissue of a human diabetes cohort decreases with total fat mass, but is not associated with measures of insulin resistance (e.g. HOMA). Together, these data indicate that FSP27 binds to lipid droplets and regulates their enlargement.

The CIDE (Cell Death-Inducing DNA Fragmentation Factor- $\alpha$ -Like Effector) family of proteins share sequence similarity with DNA fragmentation factors and were initially characterized as mitochondrial activators of apoptosis (1,2). However, strong metabolic phenotypes of mice lacking *Cidea* and *Cideb* indicate that this family plays critical roles in

energy balance (3,4). *Cidea*-knockout mice are lean and resistant to diet-induced obesity due to increased lipolysis and mitochondrial uncoupling in brown adipose tissue (3). Although expression of *Cidea* is limited to brown adipocytes in mice, humans express CIDE-A in white adipose tissue, where lower levels are observed with obesity and insulin resistance (5,6). While a coding variant of CIDE-A, V115F, is associated with human obesity (7), knockdown of CIDE-A in human adipocytes enhances lipolysis (5). *Cideb*-knockout mice are also lean and resistant to diet-induced obesity; however, this family member is expressed highly in liver, and the phenotype is due to decreased hepatic lipogenesis, increased fatty acid oxidation, and increased whole body energy expenditure (4). Thus, through a number of mechanisms, the CIDE family appears to have important roles in lipid metabolism.

Fat-specific protein of 27 kDa (FSP27 or *Cidec*) is the third member of the CIDE family. FSP27 was identified prior to the other family members based upon induction during adipogenesis (8). CIDE-3, the human version of FSP27, was characterized as 66% homologous to mouse and as an activator of apoptosis when expressed in 293T cells (9). However, the lack of function ascribed to FSP27 limited its investigation. Hepatic FSP27 is induced highly in steatotic livers that express PPAR $\gamma$ 1, providing evidence for a possible metabolic function for this protein (10). While FSP27 was detected in a screen of proteins co-purifying with 3T3-L1 adipocyte lipid droplets, suggesting that FSP27 is localized to this compartment, mitochondrial contamination of the droplets was suspected (11). Mitochondrial localization of FSP27 is consistent with findings for other CIDE family members (2,3,12) and recent mass spectrometry-based

analysis of the adipocyte proteome, which found FSP27 (Cidec) only in mitochondria (13).

Here we present evidence that FSP27 is a lipid droplet protein that plays an important role in droplet formation. Similar to members of the PAT family of lipid droplet associated proteins (14-19), overexpression of FSP27 in a variety of cell types results in spontaneous lipid accumulation. While FSP27 is not required for adipogenesis or accumulation of triacylglycerol, FSP27 deficiency prevents enlargement of lipid droplets and increases mitochondrial density. This is not due to induction of brown adipogenesis because expression of uncoupling protein-1 and other markers is not elevated. Altered accumulation of lipid may be due in part to indirect effects of FSP27 on lipid and glucose metabolism; however, localization of FSP27 to the surface of lipid droplets suggests a direct structural and/or regulatory role. A recent publication from the Czech lab corroborates several of our key findings (20).

## EXPERIMENTAL PROCEDURES

*Cell culture* - 293T cells were grown in Dulbecco's Modified Eagle Medium supplemented with 10% (v/v) bovine serum, 100 U/ml penicillin, 100 mg/ml streptomycin, 292 mg/ml L-glutamine, and 1 mM sodium pyruvate (Gibco Life Technologies, Rockville, MD). 3T3-L1 preadipocytes were grown in similar growth medium but with 8% (v/v) calf serum (Atlanta Biologicals, Lawrenceville, GA). 3T3-L1 cells were induced to differentiate into adipocytes as described previously (21).  $Rb^{-/-}$  mouse embryonic fibroblasts were induced to differentiate as described (22). Staining of neutral lipid with Oil Red O was as described previously (23). Apoptosis was assessed as described previously using membrane blebbing and nuclear condensation as morphological markers (1), or TdT-mediated dUTP nick end labeling (TUNEL) analysis (24).

*Plasmids and transfections* - pEGFP-FSP27 was created by cloning FSP27 cDNA with 5' EcoRI and 3' BamHI sites upstream and in-frame with the eGFP sequence in pEGFP-N1 (Clontech, Mountain View, CA). The entire FSP27 coding region was included except for the stop codon.

FLAG-tagged FSP27-N (amino acids 1-138) and FSP27-C (amino acids 132-239) were created by PCR and cloned into pcDNA3.1(+) (Invitrogen, Carlsbad, CA) and pLNCX2 (Clontech) vectors. Plasmids were transfected into 293T cells using calcium phosphate co-precipitation (25). Briefly, the DNA mix was incubated for 5-10 minutes at room temperature and then gently added to 293T cells that had the media changed 30 minutes before adding the precipitated DNA. After 4-6 hours of incubation, cells were shocked by removing media and gently adding 3 ml 12.5% glycerol in PBS. After a two minute incubation, the glycerol solution was aspirated and 10 ml media added. Plasmids were electroporated into 3T3-L1 adipocytes as described (26).

*Retroviral transduction of 3T3-L1 cells* - For retrovirus production, 7.5  $\mu$ g DNA of each of the two packaging vectors  $\epsilon$  and  $\psi$ , along with 7.5  $\mu$ g DNA of the retroviral plasmids were transfected into 293T cells using calcium phosphate co-precipitation (25). Media from 293T cells transfected with the retroviral vectors were passed through a 0.45  $\mu$ m sterile Millipore filter into tubes containing polybrene (8  $\mu$ g/ml) and then poured onto 30-40% confluent 3T3-L1 cells. Three rounds of infection were performed; cells were grown to 70% confluence and split into selection media containing puromycin (1.75  $\mu$ g/ml) or neomycin (8  $\mu$ g/ml). Cells were cultured in selective media while sub-confluent.

*Cell labeling and microscopy* - Bright-field images of 3T3-L1 preadipocytes and adipocytes were viewed on a Zeiss Axiovert 25 microscope and photographed with a Nikon Coolpix 885 digital camera. Confocal fluorescent images of 3T3-L1 adipocytes were taken on an Olympus Fluoview 500 microscope with Fluoview 500 software, under 60X magnification. The electroporated adipocytes were prepared as described (26) except they were fixed with 4% (w/v) paraformaldehyde (Sigma-Aldrich, St. Louis, MO) in PBS; they were stained with Oil Red O as described (23) or MitoTracker Deep Red 633 (Molecular Probes, Eugene, OR) according to the manufacturer's instructions.

293T cells were cultured on glass coverslips (Corning Inc., Corning, NY), fixed by

submersing coverslips in 4% paraformaldehyde, and permeabilized in 0.05% (w/v) Saponin (Sigma-Aldrich) in PBS. Lipids were stained with 1  $\mu$ g/ml Nile Red (Invitrogen). Nuclei were labeled by placing coverslips onto glass slides with Prolong Gold Anti-Fade with DAPI (Molecular Probes, Eugene, OR). Coverslips were dried and sealed to the slides with clear nail polish (Sally Hansen, Farmingdale, NY) and viewed on an Olympus Fluoview 500 microscope as above.

FSP27-knockdown and control adipocytes were viewed under a Philips CM-100 transmission electron microscope and photographed with a Kodak 1.6 Megapixels camera. The adipocytes were prepared for electron microscopy by fixing them for 30 min. at 4° C in 2.5% glutaraldehyde in 0.1 M Sorenson's buffer, treating with 1% osmium tetroxide in 0.1 M Sorenson's buffer for 15 min., *en bloc* staining with 3% uranyl acetate in dH<sub>2</sub>O for 15 min., dehydrating for 3 minutes each in 50%, 70%, 90%, and 100% ethanol, and then infiltrating with Epon resin according to this schedule: a 3:1 mix of ethanol:resin for 20 minutes; 1:1 ethanol:resin for 20 minutes; 1:3 ethanol:resin for 45 minutes; and 100% resin for 1 hour. The 100% resin was then refreshed and allowed to polymerize at 60° C for 24 hours. The blocks were cut into 70-nm sections with a diamond knife. The sections were placed on copper grids and stained with uranyl acetate and lead citrate for visualization of cellular components.

Electron micrographs of 3T3-L1 adipocytes were analyzed for TAG content with ImageJ software (Research Services Branch, National Institutes of Health, Bethesda, MD).

*Stable knockdown of FSP27 in 3T3-L1 adipocytes* - Four different 21-nt short hairpin RNA (shRNA) constructs targeting FSP27 mRNA were designed using Invitrogen's web-design (www.invitrogen.com). The sense oligonucleotides were FSP27-KD1: 5'-GGAAGGTTTCGCAAAGGCATCA-3'; FSP27-KD2: 5'-GCCAACTAAGAAGATCGATGT-3'; FSP27-KD3: 5'-GCAACCCTCTATGACACATAC-3'; FSP27-KD4: 5'-GGATGCCACCGAGGAAGAACA-3'. The oligonucleotides were cloned into the retroviral pSUPERIOR.retro.puro vector from OligoEngine (Seattle, WA) with a sense-loop-

antisense design, using the loop sequence CTTCTGTCA. The sense and antisense strands of the oligonucleotides (250 pmol each) were annealed in 0.1 M Tris (pH 7.5) and 1 M NaCl (50  $\mu$ l) with conditions of 95°C for 3 min, then 25 cycles of 20 seconds with a 1°C decrement per cycle, 70°C for 10 minutes and then 65 cycles of 20 seconds with a 1°C decrement per cycle, then 4°C. Annealed oligonucleotides were ligated into the pSUPERIOR.retro.puro vector using T<sub>4</sub> DNA Ligase (Invitrogen). The vector was digested with BglIII and HindIII and gel purified. Ligation was performed using 1  $\mu$ l of the annealed oligonucleotide mix, 75 ng of digested vector, T<sub>4</sub> DNA ligase and 1X ligation buffer in a 10  $\mu$ l reaction. Ligation was performed at conditions of 100 cycles of 22°C for 20 seconds and 12°C for 1 minute. The ligation mix was transformed into chemically competent DH5 $\alpha$  cells. Purified plasmids were sequenced by the core facility at the University of Michigan to verify the correct insert.

The knockdown of FSP27 expression was measured after day 10 of differentiation. FSP27 expression was measured using quantitative PCR with the forward primer 5'-GACCTCCTGAACAAGGTCCA-3' and the reverse primer 5'-TAGCTGGGCTCTCTTCTTGC-3' and SYBRGreen mastermix. Of the four shRNAs evaluated, KD1 and KD4 decreased expression of FSP27 by 85 and 65%, respectively. Results presented here are from KD1. Adipocytes with FSP27 deficiency due to KD4 showed characteristics intermediate between control and KD1 cells.

*Quantitative PCR* - Marker genes for white adipose tissue or brown adipose tissues were evaluated: Cidea, Prdm16, Cox7a1, Zic1, Tbx15, Wnt4, IGFBP3, Dpt, Aldh1a1, Meox2, FABP4, and UCP-1, PPAR $\gamma$ , C/EBP $\alpha$ , adiponectin, perilipin, ADRP and S3-12. Primers were obtained from published reports (27,28) or were designed using the Universal probe library from Roche, assay-on-demand (Applied Biosystems) or Primer Express 2.0 (Applied Biosystems). Primer sequences can be obtained upon request. RNA was harvested from cells in triplicates using TRIzol (Invitrogen) according to manufacturer's instructions. Pelleted RNAs were dissolved in 15

$\mu\text{l}$  DEPC-treated water and concentration measured with a spectrophotometer. Two  $\mu\text{g}$  RNA was reverse transcribed to cDNA using TaqMan reagents (Applied Biosystems, Foster City, CA) according to the manufacturer's protocol. Random hexamers were used for first strand cDNA synthesis. Gene expression levels were analyzed by quantitative PCR in an ABI-PRISM<sup>®</sup> 7900 Sequence Detection system (Applied Biosystems) using SYBRGreen mastermix (Applied Biosystems). Gene expression levels were normalized to 18S rRNA (pre-developed Taqman assay, Applied Biosystems). Gene expression levels for 18S were determined using the Universal PCR master mix (Applied Biosystems). All reactions were run under singleplex conditions. Samples were run in triplicates under quantitative PCR conditions. Data were quantified and normalized using the  $\Delta\text{Ct}$  method. Data are from day 14 3T3-L1 adipocytes and are representative of three independent experiments, each performed in triplicate. As controls, mRNA from mouse interscapular brown adipose tissue and cultured brown adipocytes differentiated *in vitro* were included in the real-time PCR. RNAs from cultured brown adipocytes were a present from Jamie A. Timmons and were obtained as described by Scheele et al. (29).

*Glucose uptake assay* - Day 14-16 adipocytes were incubated for three hours in serum- and glucose-free media. Basal and insulin-induced (100 nM) glucose uptake was measured by rinsing cells and incubating for 30 minutes in uptake buffer with or without insulin followed by addition of unlabeled glucose and radio-labeled 2-deoxy-D[1-<sup>3</sup>H]glucose. Cells were incubated for 20 minutes at room temperature, media was removed and cells washed in cold saline solution (0.9% NaCl). Cells were lysed in 500  $\mu\text{l}$  0.05 N NaOH and 400  $\mu\text{l}$  were added to a scintillation vial and tritium detected by addition of 3 ml Ultima Gold scintillation liquid. Protein content was measured from the remaining cell lysate using the Bio-Rad Protein assay. Glucose uptake is expressed as mean  $\pm$  S.D. and relative to control cells for each independent experiment ( $n = 5$ , each experiment performed in triplicate).

*$\beta$ -Oxidation assay* – Mitochondrial  $\beta$ -oxidation of [9,10( $n$ )<sup>3</sup>H]-palmitic acid (GE Healthcare Life Sciences, Piscataway, NJ) in 3T3-L1 preadipocytes was assayed by the degree of incorporation of <sup>3</sup>H into H<sub>2</sub>O. Krebs–Ringer buffer (Sigma-Aldrich) containing 10 mg/ml fatty acid-free BSA (Roche Applied Science, Indianapolis, IN), 100  $\mu\text{M}$  unlabeled palmitic acid (Sigma-Aldrich), and 8.33  $\mu\text{Ci/ml}$  <sup>3</sup>H-palmitic acid was added to cells that had been washed with PBS. “Blank” plates were obtained by incubating cells with methanol for one minute prior to addition of reaction mixture. Cells were incubated for two hours, then washed twice with 1 ml PBS, and the reaction mixtures and PBS were all added to NaOH-treated AG 1-X8 anion-exchange resin (Bio-Rad) in plastic chromatography columns (Evergreen Scientific, Los Angeles, CA). The resin was then washed twice with 1 ml H<sub>2</sub>O. Reaction mix, PBS, and H<sub>2</sub>O were collected in scintillation vials and <sup>3</sup>H counted for five minutes. Tritium (cpm) for the non-blank plates was normalized to the base readings from the “blank” plates, and these values were normalized to the protein concentration of each plate. After PBS washes, each plate was lysed in Lysis Buffer (1% SDS, 60 mM Tris base, 10 mM EDTA, pH 6.8) and protein concentration determined with the Bio-Rad Protein Assay.

*Triacylglycerol content* – Concentration of triacylglycerol in preadipocytes was determined using Infinity triglyceride reagent (Sigma-Aldrich) as described (30). Concentration of TAG in control and FSP27-knockdown adipocytes was determined using the GPO-Trinder Reagent (Pointe Scientific, Canton, MI), according to manufacturer's instructions. Protein concentrations were measured as described above.

*Lipolysis assay* - Day 14–17 3T3-L1 adipocytes were incubated in low-glucose media without serum but with 1% free fatty acid-free BSA (Roche Applied Science) for one hour. Media was stored at -80°C until analysis. Samples were analyzed for glycerol and non-esterified fatty acid content using the GPO-Trinder Reagent (Pointe Scientific, Canton, MI) and the half-micro NEFA C assay (WAKO Chemicals, Neuss, Germany), respectively. Samples were analyzed according to

manufacturer's instructions. Glycerol and non-esterified fatty acid release is expressed in mmol per well. Data is presented as mean  $\pm$  S.D. of three independent experiments performed in triplicates.

*Western blots* – Cultured cells were washed with PBS, lysed, and quantitated as above. Protein was separated on 4-12% gradient Tris-glycine gels and blotted onto nitrocellulose or PVDF membranes, blocked in 5% skim milk and detected with either of the following primary antibodies: PPAR $\gamma$  (Santa Cruz Biotechnology, Santa Cruz, CA); Glut4 (Chemicon, Temecula, CA); FABP4 (gift from D. Lane, Johns Hopkins University); perilipin (donated by D. Brasaemle). FABP4 and Glut4 primary antibodies were detected with HRP-coupled goat-anti-rabbit secondary antibodies (Dako) using autoradiography film. PPAR $\gamma$  and perilipin antibodies were detected by IRDye secondary antibodies and scanned on an Odyssey Infrared Imaging System (LI-COR, Lincoln, NE).

*Human diabetes study* - We used a cross-sectional case-control study design. Participants were divided into four distinct groups: patients classified as non-obese (BMI;  $<30 \text{ kg/m}^2$ ) or obese (BMI;  $\geq 30 \text{ kg/m}^2$ ) and either with normal glucose tolerance, impaired glucose tolerance, or with type 2 diabetes. Participants ( $n = 192$ ) were recruited by advertising in a local newspaper. The World Health Organization diagnostic criteria for type 2 diabetes were used to classify patients. Participants were carefully screened to isolate metabolic conditions other than type 2 diabetes. Exclusion criteria were: treatment with insulin, recent or ongoing infection and history of malignant disease. Participants were categorized as having cardiovascular disease if they had claudication or at least one of the following diagnoses: cerebrovascular accident, angina pectoris, or prior coronary artery bypass graft or percutaneous transluminal coronary angioplasty. Participants received oral and written information about the experimental procedures before giving their written informed consent. The study was approved by the Ethical Committee of Copenhagen and Frederiksberg Council (01-141/04).

*Protocol* - Participants reported in the laboratory between 0800h and 1000h after an overnight fast. They did not take any medication in the 24 h preceding the examination, and those with type 2 diabetes did not take hypoglycemic medication for one week prior to the examination. A general health examination was performed. Sphygmomanometric measurement of brachial blood pressure was performed on the participants while resting in supine position. Fasting blood samples were drawn from an antecubital vein and an oral glucose tolerance test (OGTT) performed. Prior to the OGTT, adipose tissue biopsies were obtained from abdominal subcutaneous adipose tissue using the percutaneous needle biopsy technique with suction, preceded by a subcutaneous injection of lidocaine. The biopsies were cleaned of connective tissue and blood and quickly frozen in liquid nitrogen. RNA was extracted using TRIzol (Invitrogen) according to manufacturer's instructions. Pelleted RNA was dissolved in 15  $\mu\text{l}$  DEPC-treated water and cDNA prepared as described above. Human FSP27 (CIDE-3) expression levels were normalized to the housekeeping gene GAPDH (PDAR, Applied Biosystems), and ratios of FSP27/GAPDH expression was determined using the standard curve method.

*Oral glucose tolerance test* - Blood samples were drawn before, and 1 and 2 h after drinking 500 ml of water containing 75 g of dissolved glucose. The World Health Organization diagnostic criteria were applied, i.e. normal glucose tolerance (NGT,  $n=81$ ) was defined as fasting venous plasma glucose  $<7.0$  and venous plasma glucose  $<7.8$  mM, 2 h after the oral glucose load; impaired glucose tolerance (IGT,  $n=30$ ) was defined as fasting venous plasma glucose  $<7.0$  mM and venous plasma glucose between 7.8 and 11.0 mM 2 h after the oral glucose load; type 2 diabetes (DM2,  $n=81$ ) was defined as fasting venous plasma glucose  $>7$  mM or venous plasma glucose  $>11.1$  mM 2 h after the oral glucose load. The homeostasis model assessment (HOMA) was calculated from fasting glucose and insulin measurements, and used as an indicator of insulin resistance (HOMA-IR).

*Statistical analysis* - Data from cell culture experiments were tested for significance by

ANOVA using SigmaStat 2.03. If data failed to show a normal distribution even after transformation, an ANOVA on ranks using the Mann-Whitney t-test was performed. The glucose uptake data were log-transformed to obtain a normal distribution, and data are thus presented as geometric mean  $\pm$ SD. Statistical analysis of gene expression data were performed on  $\Delta$ Ct levels (Ct-18S), which were normally distributed and thus presented as mean  $\pm$ SD. For analysis of glycerol and nonesterified fatty acid release, data were analyzed using ANOVA or ANOVA on ranks. Data are thus presented as mean  $\pm$ SD. Data from the human diabetes cohort was analyzed using SAS 9.1.

## RESULTS

*Expression of FSP27 stimulates apoptosis in 293T and 3T3-L1 cells.* To investigate the pro-apoptotic properties of FSP27, we transiently transfected 293T cells with control vector (pcDNA3.1), or expression vectors for FSP27 (including N- and C-terminal regions), death receptor 4, or Cideb (Fig. 1A). In blinded experiments, control cells underwent apoptosis at a rate of  $\sim$ 1%, while expression of FSP27 increased apoptosis to  $\sim$ 7.5%, consistent with data reported previously with the human homolog of FSP27 (9). Positive controls, death receptor 4 and Cideb, stimulated apoptosis to  $\sim$ 50 and  $\sim$ 20%, respectively. Enforced expression of either the N- or C-terminal portions of FSP27 localized the induction of apoptosis to the C-terminus (Fig. 1A). To determine whether FSP27 stimulates apoptosis in a more physiological model, 3T3-L1 cells were transduced with control or FSP27-expressing retroviruses. While differences were not seen in spontaneous apoptosis, it is likely that preadipocytes expressing high levels of FSP27 underwent apoptosis during the antibiotic selection process for retrovirus-infected cells. However, 3T3-L1 preadipocytes that ectopically express FSP27 have increased susceptibility to apoptosis as induced by serum deprivation (Fig. 1B), and day four 3T3-L1 adipocytes have increased rates of apoptosis in response to TNF $\alpha$  (Fig. 1C). Again, it is the C-terminus of FSP27 that is sufficient to stimulate apoptosis (Fig. 1C). It

should be noted that the apoptosis data from FSP27, Cideb, and death receptor 4 are not directly comparable as the relative expression levels of each protein could not be readily quantified. Nonetheless, taken together, these data suggest that exogenous expression of FSP27 is capable of stimulating apoptosis. Our results complement a recently published study that found FSP27 to promote DNA laddering and caspase-dependent proteolysis in 293T cells and visual hallmarks of apoptosis in 3T3-L1 preadipocytes (31). However, the physiological importance of these findings is unclear as mature adipocytes, which express high levels of endogenous FSP27, are quite resistant to apoptotic stimuli.

*FSP27 stimulates formation of triacylglycerol droplets.* Previous reports indicate that FSP27 is highly expressed in both white and brown adipose tissue (3) and is induced during differentiation of the TA1 adipocyte cell line (8), suggesting a functional role in adipocyte biology. Using quantitative PCR (Fig. 2A) and RNase protection assays (Fig. 2A; inset), we observed that FSP27 mRNA is also induced during differentiation of 3T3-L1 preadipocytes. While investigating the ability of FSP27 to stimulate apoptosis (Fig. 1), we observed that ectopic expression of FSP27 stimulates formation of lipid droplets in subconfluent 3T3-L1 preadipocytes (Fig. 2B). Staining of lipid droplets with Oil Red O indicates they contain neutral lipids, whereas preadipocytes expressing vector alone do not accumulate neutral lipid (Fig. 2B). FSP27 also stimulates lipid accumulation in other cell types including subconfluent NIH-3T3 cells and mouse embryonic fibroblasts (not shown). Although ectopic expression of FSP27 did not increase size of lipid droplets in 3T3-L1 adipocytes, enforced expression of FSP27 in a brown adipocyte model, *Rb*<sup>-/-</sup> mouse embryonic fibroblasts (22), dramatically increases size of lipid droplets after induction of differentiation (Fig. 2C). Similar to results observed with apoptosis, the C-terminal half of FSP27 is sufficient to stimulate lipid accumulation, whereas the N-terminal fragment had minimal droplet-inducing activity, as evidenced by an abundance of round, bright lipid droplets in 3T3-L1 preadipocytes stably expressing the C-terminus of FSP27 (Supplementary Figure 1). Finally, expression of

another member of this family (Cidea) also increases spontaneous formation of neutral lipid droplets in 3T3-L1 preadipocytes (Fig. 2B).

Spontaneous lipid accumulation in dividing preadipocytes is rare, but has been observed previously with genetic interventions that stimulate adipogenesis (32) or increase expression of perilipin or adipophilin (14-19). To determine whether lipid accumulation in response to FSP27 is due to stimulation of preadipocyte differentiation, we lysed 3T3-L1 preadipocytes and observed by immunoblot that expression of FABP4 is not induced in the FSP27-expressing cells (Fig. 2D). In addition, we also observed that expression of C/EBP $\alpha$  and PPAR $\gamma$  mRNAs was unaltered (data not shown).

To evaluate the nature of the accumulated neutral lipid, we measured total TAG and observed a significant increase in 3T3-L1 preadipocytes expressing FSP27 (Fig. 2E). Although FSP27 does not increase the low rate of incorporation of [ $^{14}$ C]-acetate into TAG observed in preadipocytes (data not shown), expression of FSP27 decreases oxidation of tritiated palmitic acid to water (Fig. 2F), suggesting that FSP27 either regulates oxidation of fatty acids, or FSP27 is involved in diverting fatty acids into TAG droplets.

*FSP27 localizes to triacylglycerol droplets.* Given the ability of FSP27 to cause lipid droplet formation in a variety of cultured cells, we hypothesized that FSP27 is a mitochondrial protein, like Cidea (3), that decreases fatty acid oxidation. To evaluate cellular localization, we created a vector that expresses an FSP27-eGFP fusion gene. Consistent with the eGFP-fusion protein retaining activity of FSP27, transfection of 293T cells with pEGFP-FSP27 stimulates accumulation of lipid droplets (Fig. 3B). When 293T cells are labeled with the nuclear dye 4',6-diamidino-2-phenylindole (DAPI) and the neutral lipid dye Nile red, the FSP27-eGFP fusion protein is largely localizes to cytoplasmic lipid droplets (Fig. 3B). As in previous reports, eGFP alone is distributed throughout the cell (Fig. 3A), and we did not observe lipid droplets. To verify this compartmentalization of FSP27 in an adipocyte-like cell line, we transfected mature 3T3-L1 adipocytes with pEGFP-FSP27 by electroporation.

We again observed FSP27-eGFP primarily around lipid droplets, labeled with Oil Red O, though non-droplet GFP fluorescence can clearly be seen (Fig. 3C, top row), leading us to speculate that FSP27-eGFP overexpression caused artifactual expression in one or more compartments. We therefore labeled adipocytes with MitoTracker Deep Red 633 to assess the colocalization of FSP27-eGFP and mitochondria. We typically observed a circular GFP expression pattern that did not coincide with MitoTracker (Fig 3C, bottom row), indicating FSP27-eGFP is largely a lipid droplet-binding protein. In contrast, adipocytes transfected with pEGFP-N1 alone had only a nuclear GFP signal (not shown).

*FSP27 deficiency in 3T3-L1 adipocytes inhibits formation of large lipid droplets.* To investigate the effects of endogenous FSP27 deficiency on cell morphology, gene expression, and metabolism, we stably “knocked down” expression of FSP27 in 3T3-L1 cells using a retroviral shRNA approach. As FSP27 mRNA is induced substantially at day three of adipogenesis (Fig. 2A), it is not surprising that the effect of FSP27 deficiency in 3T3-L1 cells became apparent only after cells were induced to differentiate. Measurement of FSP27 mRNA in Day 14 adipocytes revealed that four independent shRNA constructs decreased expression by 50% to 85% (Fig. 4A; data not shown). The KD1 cells had an ~85% knockdown of FSP27, and while these cells accumulated many small lipid droplets during adipogenesis, these did not mature into the larger lipid droplets observed in control 3T3-L1 adipocytes (Fig. 4B). KD4 decreased expression of FSP27 by ~65% and caused seemingly identical morphological changes, but only in 60–70% of the cells, consistent with the level of knockdown (not shown). The other two lines did not show morphological changes, suggesting a threshold for FSP27 deficiency must be attained for phenotypic effects. The adipocytes in KD1 cells are not incapable of storing lipid *per se*, as Oil Red-O staining reveals substantial TAG in FSP27-deficient adipocytes (Fig. 4C) and enzymatic assays indicate similar TAG levels between control and FSP27-KD adipocytes (in one representative experiment, scrambled =  $3.8 \pm 0.74$   $\mu$ mol TAG/mg protein and FSP27-KD1 =  $5.7 \pm$

1.81  $\mu\text{mol TAG/mg protein}$ ;  $p = 0.23$ ). Instead, the defect appears to be at the level of lipid droplet enlargement.

To gain better insight into the morphological changes of the FSP27-KD cells, we analyzed electron micrographs of individual adipocytes expressing the KD1 or scrambled shRNAs (Fig. 4D). In 25 cells of each genotype, FSP27-KD1 adipocytes contained an average of  $83 \pm 70$  TAG droplets per cell, whereas control adipocytes averaged only  $25 \pm 19$  ( $p < 0.001$ ) (Fig. 4E). The total area of the two-dimensional cell sections occupied by TAG, as measured with ImageJ software, did not differ between the two cell types, whether expressed as TAG area per cell or TAG area/cross-sectional area of the cell (not shown). This confirms the similarity in TAG contents obtained by enzymatic assay (see above) and indicates a primary defect in droplet enlargement and not in lipid accumulation *per se*.

Additionally, in the same 25 cells of each construct, FSP27-KD1 adipocytes contained more mitochondria per cell and per cross-sectional area of the cell than controls. (Fig. 4E). The knockdowns had approximately  $280 \pm 178$  mitochondria per cell, and the controls contained  $190 \pm 90$  mitochondria per cell ( $p < 0.05$ ).

*Effects of FSP27 deficiency on adipogenesis and metabolism.* Ectopic expression of FSP27 in preadipocytes stimulates lipid accumulation without expression of adipocyte genes (Fig. 2). Thus, we hypothesized that knockdown of FSP27 would not alter adipogenesis, and that effects would be restricted to the TAG droplets. Consistent with this idea, immunoblot analysis of day 14 adipocytes revealed no consistent difference in PPAR $\gamma$  or FABP4 expression between control and FSP27-deficient adipocytes (Fig. 5A). To determine whether FSP27 deficiency causes up-regulation of a constitutive PAT protein (33), we evaluated perilipin protein levels and found similar amounts of perilipin in control and FSP27-KD1 cells (Fig. 5A). Additionally, we performed quantitative PCR (Q-PCR) analysis on several adipocyte genes coding for proteins involved in adipocyte differentiation and metabolism and lipid droplet binding. We found that mRNA levels of PPAR $\gamma$ , C/EBP $\alpha$ , adiponectin (Adipoq), perilipin, adipophilin (ADRP), S3-12, FABP4, and Glut1 were similar

between control and FSP27-KD1 cells (Fig. 5B). These protein and mRNA expression data suggest morphological changes associated with FSP27 deficiency are not due to impaired adipocyte differentiation. We observed significant upregulation of cytochrome *c* oxidase subunit VIIa polypeptide 1 (Cox7a1), a component of the mitochondrial respiratory chain, in FSP27-KD1 adipocytes (Fig. 5B), lending some support to our finding of increased mitochondrial number in FSP27-deficient adipocytes.

Other members of the CIDE family, Cidea and Cideb, influence metabolism and whole-body lipid homeostasis (3-5,34). To investigate effects of FSP27 deficiency on metabolic variables in adipocytes, we measured basal and stimulated glucose uptake and lipolysis. While insulin-stimulated glucose uptake was not affected by knockdown of FSP27 (data not shown), basal glucose uptake was significantly elevated (Fig. 6A) despite similar levels of Glut1 mRNA (Fig. 5B) and Glut4 protein (Fig. 6B). In contrast, while this paper was in revision, another group found that RNA-interference against FSP27 increased insulin-stimulated glucose uptake and Glut4 expression (35). In addition to altered glucose metabolism, FSP27 also seems to have a moderate impact on lipid homeostasis. Glycerol release, a common index of lipolysis, exhibited a slight trend towards being increased in FSP27-KD1 adipocytes compared with the scrambled controls (Fig. 6C). The similar increases under basal and stimulated conditions suggest that signaling from adrenergic receptors through to lipases as well as glycerol export are intact in FSP27-KD1 adipocytes. In contrast, basal release of non-esterified fatty acids is similar between FSP27-deficient and control adipocytes, but increased release of fatty acids in response to isoproterenol suggests that lipolysis is slightly increased (Fig. 6D). Alternatively,  $\beta$ -oxidation or recycling of fatty acids into triacylglycerol may be decreased under these circumstances. Taken together, these data reveal a role for FSP27 in glucose and lipid homeostasis; however, these effects are likely secondary to the required role of FSP27 for expansion of lipid droplets and not directly related to regulation of adipocyte metabolism.

*Effects of FSP27 deficiency on gene expression.* Since FSP27-knockdown cells display a

phenotype of small lipid droplets that is somewhat reminiscent of brown adipose cells, we explored the possibility that FSP27 deficiency stimulates brown adipocyte development. While expression of markers specific for brown adipose tissue, such as uncoupling protein-1, Prdm16, Zic1, and Meox2, were readily detected in cultured brown adipocytes and in brown adipose tissue, neither FSP27 knockdown cells nor control cells express appreciable levels of these genes (Table 1). These data suggest that the multilocular/mitochondria-dense phenotype of FSP27-deficient adipocytes is not due to expression of brown adipocyte genes. Although expression of many white adipocyte genes is not altered by FSP27 deficiency (Fig. 5), increased expression of Cox7a1 and insulin-like growth factor binding protein-3 (IGFBP3) is observed in FSP27-KD1 adipocytes (Fig. 5B, Table 1). Furthermore, FSP27 deficiency is associated with decreased expression of dermatopontin, a protein involved in integrin signaling and extracellular matrix modeling, and Wnt4 (Table 1), suggesting that FSP27 deficiency may have unanticipated and far-reaching indirect effects on adipocyte biology.

*Decreased expression of FSP27 in adipose tissue of obese compared to non-obese humans.* Expression of CIDE-A mRNA is lower in adipose tissue of obese individuals (5,6). To investigate the potential regulation of FSP27 in human adipose tissue and its potential role in predicting insulin sensitivity, we measured FSP27 mRNA in a cohort consisting of obese and non-obese persons with type 2 diabetes, and obese and non-obese healthy controls (Fig. 8). After adjusting for age and sex, expression of FSP27 mRNA in subcutaneous adipose tissue correlates negatively with body mass index ( $p < 0.01$ ; data not shown) and with total fat mass (Fig. 8). There was, however, no association between FSP27 expression in subcutaneous adipose tissue and HOMA index ( $p = 0.75$ ), or resting plasma levels of insulin ( $p = 0.32$ ) or glucose ( $p = 0.88$ ). Thus, FSP27 appears to be suppressed coordinately with other adipocyte genes and/or proteins such as lipin-1 $\beta$ , adipose triglyceride lipase, aquaporin-7, and SREBP1c involved in lipid metabolism (36-38), and unlike CIDEA (5,6), does not appear to be associated with insulin sensitivity.

## DISCUSSION

In the present study, we demonstrate that expression of FSP27, a protein mainly found in adipose tissue and markedly induced during adipogenesis *in vitro*, is sufficient to stimulate formation of lipid droplets and is necessary for expansion of lipid droplet size during adipogenesis (Fig. 1-4). Recent work from Puri et al. (20) also indicates that expression of FSP27 is required to maintain large lipid droplets in mature adipocytes. FSP27 has several characteristics in common with the PAT family, which was originally defined as perilipin, adipophilin, and tail-interacting protein of 47 kDa (TIP47), but which now includes other validated members such as S3-12 (39) and myocardial lipid droplet protein/lipid storage droplet protein-5/PAT-1 (18,40,41). As observed previously with perilipin and adipophilin (14-19), expression of exogenous FSP27 in a variety of cell types stimulates the spontaneous accumulation of triglyceride-containing lipid droplets (20; Fig. 2, 3), a characteristic also shared with Cidea (Fig. 2). Similar to the PAT proteins, FSP27-eGFP fusion proteins localize to lipid droplet surfaces in 293T cells and cultured adipocytes (Fig. 3), suggesting a structural and/or regulatory role for lipid droplet formation.

While the basis for association of FSP27 with lipid droplets has not been investigated, binding to the lipid droplet surface or binding to other droplet-associated proteins are both plausible. A protein (hetero- and homo-dimer) interaction domain has been investigated in the CIDE family but this resides at the N-terminus (2). Thus, dimer formation is not likely important in this regard given our finding that the C-terminus of FSP27 is sufficient to stimulate lipid droplet formation in 3T3-L1 preadipocytes (Supplementary Figure 1). Although interactions with CIDE proteins have not been reported, adipophilin and perilipin bind a variety of proteins (e.g. CGI-58), and also act as gatekeepers for hormone-sensitive lipase and adipocyte triglyceride lipase (16-18). In general, different droplet-associated proteins predominate on different-sized droplets in adipocytes; for instance, perilipin seems to be more concentrated on smaller lipid droplets (42). Given that FSP27 binds small droplets in 293 cells and large droplets in adipocytes (Fig. 3), interaction of FSP27 with

several members of the PAT family would be required if associations with the lipid droplet are mediated through protein-protein interactions.

Although FSP27 and Cidea share some similarities with PAT proteins, these lipid-binding PAT proteins compensate for each other's loss, with adipophilin binding to lipid droplets in the absence of perilipin (43), and TIP47 associating with lipid droplets in the absence of adipophilin (44)—with the net effect that lipid droplet size is not influenced by the absence of these PAT proteins in cultured cells. In contrast, FSP27 deficiency during adipogenesis prevents the formation of large lipid droplets, although considerable triacylglycerol accumulates in the form of numerous smaller lipid droplets (20; Fig. 4). In addition, compensatory up-regulation of Cidea, adipophilin, S3-12 or perilipin mRNAs, or perilipin protein was not observed in FSP27-deficient adipocytes (Fig. 5). Like PAT proteins (19,45), FSP27 does not influence adipogenesis, as assessed by expression of several white and brown adipocyte genes (Fig. 5; Table 1); however, FSP27 clearly has unique roles in lipid droplet biology.

Lipid droplet-associated proteins can also play important roles in the regulation of lipid metabolism. For example, in response to adrenergic stimuli, phosphorylation of perilipin is thought to allow docking of hormone-sensitive lipase, for access to the interior of the lipid droplet (42,46). Thus, adipocytes from perilipin knockout mice have a 10-fold increase in basal lipolysis, while isoproterenol-stimulated lipolysis is attenuated, and the animals accordingly have less adipose tissue (19,45). Conversely, expression of perilipin in 3T3-L1 preadipocytes prevents lipolysis by shielding the lipid droplet from lipases (14). In contrast to perilipin, FSP27 knockdown cells release glycerol normally in response to isoproterenol, suggesting that FSP27 is not involved in regulated lipolysis. After stimulation with isoproterenol, increased non-esterified fatty acid release without elevated glycerol suggests that FSP27 may influence recycling of fatty acids. Knockdown of the FSP27 homologue CIDE-A enhances glycerol release from cultured human adipocytes, providing further support for regulation of lipolysis by this family of proteins (5). While the decrease in  $\beta$ -oxidation of fatty acids observed with ectopic expression of FSP27 in 3T3-L1 preadipocytes (Fig. 2) is consistent with

mitochondrial localization and regulation of uncoupling, as suggested by prior work with Cidea (3), localization of FSP27 to the lipid droplet favors a mechanism where FSP27 redirects flux of tritiated fatty acids into stored triacylglycerol (20; Fig. 3).

Given the phenotype of many small droplets exhibited by FSP27-KD adipocytes, we were surprised they did not have substantially higher rates of lipolysis than controls. With the much greater total surface area of lipid droplets in these cells, the knockdowns must have lower rates of lipolysis per surface area of TAG. This has intriguing implications for the as-yet undiscovered functions of FSP27; for instance, while its absence could to some extent promote lipolysis via increased exposed area of TAG, the protein could also play a facilitative role in the access of lipases to TAG, like perilipin (42,46), leading to reduced lipolytic rates as a function of droplet surface area when FSP27 expression is reduced.

We were particularly intrigued by our finding of higher mitochondrial number in FSP27-knockdown adipocytes compared to wild-type adipocytes. It is too early to determine whether the increased mitochondria are a direct effect of FSP27 deficiency or an indirect result of smaller lipid droplets. Our data (Fig. 3) and recently published work (20) showing lipid droplet localization of FSP27, in addition to our evidence that a brown adipocyte phenotype is not induced in FSP27-KD adipocytes (Table 1), suggest that increased mitochondrial number indirectly results from defects in droplet enlargement.

It is tempting to speculate that FSP27 has importance in the pathophysiology of obesity in humans. Both FSP27 and CIDE-A are expressed in human white adipose tissue, and similar to a group of adipocyte genes involved in lipid homeostasis (36-38), expression correlates negatively with body mass index and total fat mass (Figure 7). However, in contrast to CIDE-A in adipose tissue (5) and adipophilin in skeletal muscle (47), FSP27 mRNA levels are not associated with insulin resistance as determined by HOMA-IR index, or fasting blood insulin or glucose levels, thus negating a role for FSP27 gene expression in insulin resistance in this Danish cohort. Although FSP27 is generally expressed in adipocytes, high levels are also observed in steatotic livers (31,48; data not shown), suggesting

a causative role in hepatic lipid accumulation. Cidea and adipophilin are also highly expressed in steatotic liver (34,40,49-51) where they as well as Cideb are involved in hepatic lipid accumulation (4,52,53); however, additional experiments are required to test a role for FSP27 in hepatic steatosis.

## REFERENCES

1. Inohara, N., Koseki, T., Chen, S., Wu, X., and Nunez, G. (1998) *Embo J* **17**(9), 2526-2533
2. Inohara, N., Koseki, T., Chen, S., Benedict, M. A., and Nunez, G. (1999) *J. Biol. Chem.* **274**(1), 270-274
3. Zhou, Z., Yon Toh, S., Chen, Z., Guo, K., Peng Ng, C., Ponniah, S., Lin, S.-C., Hong, W., and Li, P. (2003) *Nat Genet* **35**(1), 49-56
4. Li, J. Z., Ye, J., Xue, B., Qi, J., Zhang, J., Zhou, Z., Li, Q., Wen, Z., and Li, P. (2007) *Diabetes*, db07-0040
5. Nordstrom, E. A., Ryden, M., Backlund, E. C., Dahlman, I., Kaaman, M., Blomqvist, L., Cannon, B., Nedergaard, J., and Arner, P. (2005) *Diabetes* **54**(6), 1726-1734
6. Gummesson, A., Jernas, M., Svensson, P.-A., Larsson, I., Glad, C. A. M., Schele, E., Gripeteg, L., Sjöholm, K., Lystig, T. C., Sjöström, L., Carlsson, B., Fagerberg, B., and Carlsson, L. M. S. (2007) *J Clin Endocrinol Metab*, jc.2007-1136
7. Dahlman, I., Kaaman, M., Jiao, H., Kere, J., Laakso, M., and Arner, P. (2005) *Diabetes* **54**(10), 3032-3034
8. Danesch, U., Hoeck, W., and Ringold, G. M. (1992) *J. Biol. Chem.* **267**(10), 7185-7193
9. Liang, L., Zhao M, Xu Z, Yokoyama KK, Li T. (2003) *Biochemical Journal* **370**(1), 195-203
10. Sato, W., Horie, Y., Kataoka, E., Ohshima, S., Dohmen, T., Iizuka, M., Sasaki, J., Sasaki, T., Hamada, K., and Kishimoto, H. (2006) *Hepatology Research* **34**(4), 256-265
11. Brasaemle, D. L., Dolios, G., Shapiro, L., and Wang, R. (2004) *J Biol Chem* **279**(45), 46835-46842
12. Chen, Z., Guo, K., Toh, S. Y., Zhou, Z., and Li, P. (2000) *J. Biol. Chem.* **275**(30), 22619-22622
13. Adachi, J., Kumar, C., Zhang, Y., and Mann, M. (2007) *Mol Cell Proteomics* **6**(7), 1257-1273
14. Brasaemle, D. L., Rubin, B., Harten, I. A., Gruia-Gray, J., Kimmel, A. R., and Londos, C. (2000) *J. Biol. Chem.* **275**(49), 38486-38493
15. Imamura, M., Inoguchi, T., Ikuyama, S., Taniguchi, S., Kobayashi, K., Nakashima, N., and Nawata, H. (2002) *Am J Physiol Endocrinol Metab* **283**(4), E775-783
16. Londos, C., Sztalryd, C., Tansey, J. T., and Kimmel, A. R. (2005) *Biochimie* **87**(1), 45-49
17. Listenberger, L. L., Ostermeyer-Fay, A. G., Goldberg, E. B., Brown, W. J., and Brown, D. A. (2007) *J. Lipid Res.*, M700359-JLR700200
18. Yamaguchi, T., Matsushita, S., Motojima, K., Hirose, F., and Osumi, T. (2006) *J. Biol. Chem.* **281**(20), 14232-14240
19. Tansey, J. T., Huml, A. M., Vogt, R., Davis, K. E., Jones, J. M., Fraser, K. A., Brasaemle, D. L., Kimmel, A. R., and Londos, C. (2003) *J. Biol. Chem.* **278**(10), 8401-8406
20. Puri, V., Konda, S., Ranjit, S., Aouadi, M., Chawla, A., Chouinard, M., Chakladar, A., and Czech, M. P. (2007) *J. Biol. Chem.*, M707404200
21. Student, A. K., Hsu, R. Y., and Lane, M. D. (1980) *J. Biol. Chem.* **255**(10), 4745-4750
22. Hansen, J. B., Jorgensen, C., Petersen, R. K., Hallenborg, P., De Matteis, R., Boye, H. A., Petrovic, N., Enerback, S., Nedergaard, J., Cinti, S., Riele, H. t., and Kristiansen, K. (2004) *PNAS* **101**(12), 4112-4117
23. Preece, A. (1972) *A Manual for Histologic Technicians*, Little Brown, Boston
24. Longo, K. A., Kennell, J. A., Ochocinska, M. J., Ross, S. E., Wright, W. S., and MacDougald, O. A. (2002) *J. Biol. Chem.* **277**(41), 38239-38244
25. Jordan, M., Schallhorn, A., and Wurm, F. M. (1996) *Nucl. Acids Res.* **24**(4), 596-601

26. Chiang, S., Chang, L., Saltiel, A. R., and William E. Balch, C. J. D. a. A. H. (2006) TC10 and Insulin[hyphen (true graphic)]Stimulated Glucose Transport. In. *Methods in Enzymology*, Academic Press
27. Timmons, J. A., Wennmalm, K., Larsson, O., Walden, T. B., Lassmann, T., Petrovic, N., Hamilton, D. L., Gimeno, R. E., Wahlestedt, C., Baar, K., Nedergaard, J., and Cannon, B. (2007) *Proceedings of the National Academy of Sciences* **104**(11), 4401-4406
28. Seale, P., Kajimura, S., Yang, W., Chin, S., Rohas, L. M., Uldry, M., Tavernier, G., Langin, D., and Spiegelman, B. M. (2007) *Cell Metab* **6**(1), 38-54
29. Scheele, C., Nielsen, A. R., Walden, T. B., Sewell, D. A., Fischer, C. P., Brogan, R. J., Petrovic, N., Larsson, O., Tesch, P. A., Wennmalm, K., Hutchinson, D. S., Cannon, B., Wahlestedt, C., Pedersen, B. K., and Timmons, J. A. (2007) *FASEB J.*, fj.07-8520com
30. Ross, S. E., Erickson, R. L., Gerin, I., DeRose, P. M., Bajnok, L., Longo, K. A., Misek, D. E., Kuick, R., Hanash, S. M., Atkins, K. B., Andresen, S. M., Nebb, H. I., Madsen, L., Kristiansen, K., and MacDougald, O. A. (2002) *Mol. Cell. Biol.* **22**(16), 5989-5999
31. Kim, J. Y., Liu, K., Zhou, S., Tillison, K., Wu, Y., and Smas, C. M. (2008) *Am J Physiol Endocrinol Metab*, 00104.02007
32. Ross, S. E., Hemati, N., Longo, K. A., Bennett, C. N., Lucas, P. C., Erickson, R. L., and MacDougald, O. A. (2000) *Science* **289**(5481), 950-953
33. Wolins, N. E., Brasaemle, D. L., and Bickel, P. E. (2006) *FEBS Letters* **580**(23), 5484-5491
34. Kelder, B., Boyce, K., Kriete, A., Clark, R., Berryman, D., Nagatomi, S., List, E., Braughler, M., and Kopchick, J. (2007) *Comparative Hepatology* **6**(1), 4
35. Puri, V., Virbasius, J. V., Guilherme, A., and Czech, M. P. (2008) *Acta Physiologica* **192**(1), 103-115
36. Steinberg, G. R., Kemp, B. E., and Watt, M. J. (2007) *Am J Physiol Endocrinol Metab* **293**(4), E958-964
37. Croce, M. A., Eagon, J. C., LaRiviere, L. L., Korenblat, K. M., Klein, S., and Finck, B. N. (2007) *Diabetes* **56**(9), 2395-2399
38. Ceperuelo-Mallafre, V., Miranda, M., Chacon, M. R., Vilarrasa, N., Megia, A., Gutierrez, C., Fernandez-Real, J. M., Gomez, J. M., Caubet, E., Fruhbeck, G., and Vendrell, J. (2007) *J Clin Endocrinol Metab* **92**(9), 3640-3645
39. Wolins, N. E., Skinner, J. R., Schoenfish, M. J., Tzekov, A., Bensch, K. G., and Bickel, P. E. (2003) *J. Biol. Chem.* **278**(39), 37713-37721
40. Dalen, K. T., Dahl, T., Holter, E., Arntsen, B., Londos, C., Sztalryd, C., and Nebb, H. I. (2007) *Biochimica et Biophysica Acta (BBA) - Molecular and Cell Biology of Lipids* **1771**(2), 210-227
41. Wolins, N. E., Quaynor, B. K., Skinner, J. R., Tzekov, A., Croce, M. A., Gropler, M. C., Varma, V., Yao-Borengasser, A., Rasouli, N., Kern, P. A., Finck, B. N., and Bickel, P. E. (2006) *Diabetes* **55**(12), 3418-3428
42. Granneman, J. G., Moore, H.-P. H., Granneman, R. L., Greenberg, A. S., Obin, M. S., and Zhu, Z. (2007) *J. Biol. Chem.* **282**(8), 5726-5735
43. Tansey, J. T., Sztalryd, C., Gruia-Gray, J., Roush, D. L., Zee, J. V., Gavrilova, O., Reitman, M. L., Deng, C. X., Li, C., Kimmel, A. R., and Londos, C. (2001) *Proc Natl Acad Sci U S A* **98**(11), 6494-6499
44. Sztalryd, C., Bell, M., Lu, X., Mertz, P., Hickenbottom, S., Chang, B. H. J., Chan, L., Kimmel, A. R., and Londos, C. (2006) *J. Biol. Chem.* **281**(45), 34341-34348
45. Martinez-Botas, J., Anderson, J. B., Tessier, D., Lapillonne, A., Chang, B. H., Quast, M. J., Gorenstein, D., Chen, K. H., and Chan, L. (2000) *Nat Genet* **26**(4), 474-479
46. Sztalryd, C., Xu, G., Dorward, H., Tansey, J. T., Contreras, J. A., Kimmel, A. R., and Londos, C. (2003) *J. Cell Biol.* **161**(6), 1093-1103
47. Phillips, S. A., Choe, C. C., Ciaraldi, T. P., Greenberg, A. S., Kong, A. P. S., Baxi, S. C., Christiansen, L., Mudaliar, S. R., and Henry, R. R. (2005) *Obesity Res* **13**(8), 1321-1329

48. Yu, S., Cao, W.-Q., Kashireddy, P., Meyer, K., Jia, Y., Hughes, D. E., Tan, Y., Feng, J., Yeldandi, A. V., Rao, M. S., Costa, R. H., Gonzalez, F. J., and Reddy, J. K. (2001) *J. Biol. Chem.* **276**(45), 42485-42491
49. Li, J. Z., Ye, J., Xue, B., Qi, J., Zhang, J., Zhou, Z., Li, Q., Wen, Z., and Li, P. (2007) *Diabetes* **56**(10), 2523-2532
50. Schadinger, S. E., Bucher, N. L. R., Schreiber, B. M., and Farmer, S. R. (2005) *Am J Physiol Endocrinol Metab* **288**(6), E1195-1205
51. Motomura, W., Inoue, M., Ohtake, T., Takahashi, N., Nagamine, M., Tanno, S., Kohgo, Y., and Okumura, T. (2006) *Biochem Biophys Res Commun* **340**(4), 1111-1118
52. Imai, Y., Varela, G. M., Jackson, M. B., Graham, M. J., Crooke, R. M., and Ahima, R. S. (2007) *Gastroenterology* **132**(5), 1947-1954
53. Chang, B. H.-J., Li, L., Paul, A., Taniguchi, S., Nannegari, V., Heird, W. C., and Chan, L. (2006) *Mol. Cell. Biol.* **26**(3), 1063-1076

### FOOTNOTES

\*These authors contributed equally to this research.

This work was supported by National Institutes of Health Grant DK62876 to O.A.M. P.K. is supported by the Lundbeck Foundation and the Novo Nordisk Foundation and received a travel grant from The Danish Research Agency. J.T.P. is a Maas Fellow and is supported by the Systems and Integrative Biology Training Grant. Additional support was provided by the Michigan Metabolomics and Obesity Center. The Centre of Inflammation and Metabolism is supported by a grant from the Danish National Research Foundation (#02-512-55). The study was further supported by the Danish Medical Research Council (# 22-01-009 and # 22-03-0367). We thank Ruth Rousing, Hanne Villumsen, and Bettina Starup Mentz for their technical assistance, and James A. Timmons for help with selection criteria for adipocyte gene expression markers. We are especially grateful to Chris Edwards, Sasha Meshinchi, and Dotty Sorenson of the University of Michigan Microscopy and Image Analysis Laboratory for their help with confocal and electron microscopy and preparation of TEM sections.

The abbreviations used are: FSP27, fat specific protein 27; shRNA, short-hairpin RNA; PBS, phosphate buffered saline; PPAR $\gamma$ , Peroxisome Proliferator Activated Receptor  $\gamma$ ; FABP4, fatty acid binding protein 4; CIDE, Cell Death-Inducing DNA Fragmentation Factor- $\alpha$ -Like Effector; TAG, triacylglycerol; TEM, transmission electron microscope; HRP, horseradish peroxidase; HOMA, homeostatic model assessment.

### FIGURE LEGENDS

**Figure 1.** Overexpression of FSP27 in 293T and 3T3-L1 preadipocytes stimulates apoptosis. *A*, 293T cells were transiently co-transfected with lacZ and either control vector, or vectors directing expression of FSP27, FSP-N, FSP-C, death receptor 4 (DR4), or Cideb. Apoptosis in transfected cells was evaluated using morphological criteria 24 h later and data are presented as the percent of cells showing membrane blebbing and nuclear condensation. *B*, 3T3-L1 preadipocytes were transduced with control or FSP27-expressing retroviruses. After selection, cells were deprived of serum for 24 h. Apoptosis was evaluated by TUNEL staining and quantified with NIH Image. *C*, At day four of differentiation, the indicated adipocytes were exposed to 15 ng/ml TNF $\alpha$  and analyzed as in *B*. All data are presented as mean  $\pm$  S.D. ( $n = 6$ ). Differences between FSP27 and controls were determined using Student's t-test. \*,  $p < 0.05$ .

**Figure 2.** FSP27 stimulates accumulation of triacylglycerol and inhibits  $\beta$ -oxidation of non-esterified fatty acids. *A*, Expression of FSP27 is induced during 3T3-L1 adipogenesis. Expression during differentiation was assessed by quantitative PCR (graph) and RNase protection assay (inset). *B*, Ectopic expression of FSP27 or Cidea stimulates neutral lipid accumulation in 3T3-L1 preadipocytes, visualized by Oil Red O staining. *C*, Retroviral expression of FSP27 in  $Rb^{-/-}$  mouse embryonic fibroblasts induces larger lipid droplets. *D*, Lipid accumulation in response to FSP27 is not associated with induction of FABP4. Immunoblot for FABP4 in lysates from control and FSP27-expressing 3T3-L1 preadipocytes. Differentiated adipocytes (Ads) were included as a positive control. *E*, Total TAG content of 3T3-L1 preadipocytes infected with control (pLNCX2) or FSP27-expressing retroviruses. *F*,  $\beta$ -oxidation of  $^3\text{H}$ -palmitic acid in control (pLNCX2) or FSP27-expressing preadipocytes. Data are expressed as mean  $\pm$  S.D. ( $n = 6$ ). Differences between FSP27 and controls were determined using Student's t-test. \*,  $p < 0.05$ .

**Figure 3.** Localization of FSP27-eGFP to lipid droplets in 293T cells and 3T3-L1 adipocytes. Fluorescent images of 293T cells transfected with *A*, pEGFP-N1 or *B*, pEGFP-FSP27. Nuclei labeled with DAPI (*left panel*), neutral lipid stained with Nile red (*second panel*), location of eGFP (*third panel*), and merging of the three images (*right panel*). *C*, Confocal fluorescent images of 3T3-L1 adipocytes at day five of differentiation transfected with pEGFP-FSP27 by electroporation. Oil Red O staining (*top row, left panel*) or MitoTracker Deep Red staining (*bottom row, left panel*), GFP (*middle*), and overlay (*right*). Bar, 10  $\mu\text{m}$ .

**Figure 4.** FSP27 deficiency inhibits development of large lipid droplets and increases mitochondrial number but has no effect on adipogenesis. *A*, Knockdown of FSP27 mRNA in 3T3-L1 adipocytes stably expressing an anti-FSP27 shRNA (KD1) or a scrambled shRNA was assessed by quantitative PCR. *B*, Phase contrast microscopy of control (*left*) and FSP27-KD1 (*right*) adipocytes. *C*, Oil red-O staining of adipocytes expressing scrambled (*left*) or FSP27-KD1 (*right*) shRNAs. *D*, Transmission electron micrographs of a scrambled (*left*) or FSP27-KD1 (*right*) adipocyte. Bar, 2  $\mu\text{m}$ . *E*, Average number of mitochondria and TAG droplets per cell in scrambled (*open bars*) or FSP27-KD1 (*black bars*) adipocytes. Data are presented as mean  $\pm$  S.D. Differences between FSP27 and controls were determined using Student's t-test. \*,  $p < 0.05$ ; †,  $p < 0.001$ .

**Figure 5.** Adipogenesis and perilipin levels are not altered in FSP27-KD1 adipocytes, but mitochondrial gene expression is. *A*, PPAR $\gamma$ , FABP4, and perilipin were assessed by immunoblot in lysates from scrambled and FSP27-KD1 adipocytes. *B*, Quantitative PCR analysis of mRNAs for PPAR $\gamma$ , C/EBP $\alpha$ , adiponectin (Adipoq), perilipin, adipophilin (ADRP), S3-12, Glut1, and Cox7a1. Data are presented as mean  $\pm$  S.D. Differences between FSP27 and controls were determined using Student's t-test. †,  $p < 0.001$ .

**Figure 6.** FSP27 deficiency alters glucose uptake and lipid metabolism in 3T3-L1 adipocytes without affecting Glut4 levels. *A*, After serum deprivation for 3 h, basal glucose uptake was evaluated. *B*, Western blot of Glut4 in scrambled and FSP27-KD1 adipocytes. GAPDH, loading control. *C*, Glycerol and *D*, non-esterified fatty acid (NEFA) release from control and FSP27-KD1 adipocytes was assessed under basal conditions and after stimulation with isoproterenol for 1 h. Data are presented as mean  $\pm$  S.D. Differences between FSP27 and controls were determined using Student's t-test. \*,  $p < 0.05$ .

**Figure 7.** Decreased expression of FSP27 in adipose tissue of obese humans. RNA isolated from subcutaneous adipose tissue of a cohort of 191 non-obese or obese persons without or with type 2 diabetes was analyzed for expression of FSP27. After normalization to glyceraldehyde-3-phosphate dehydrogenase, logarithmic values of FSP27 are presented relative to total adipose tissue (kg) for each

person. Linear regression analysis reveals a negative association between FSP27 and adipose tissue mass after adjusting for age and sex ( $p = 0.0017$ ).



Figure 1

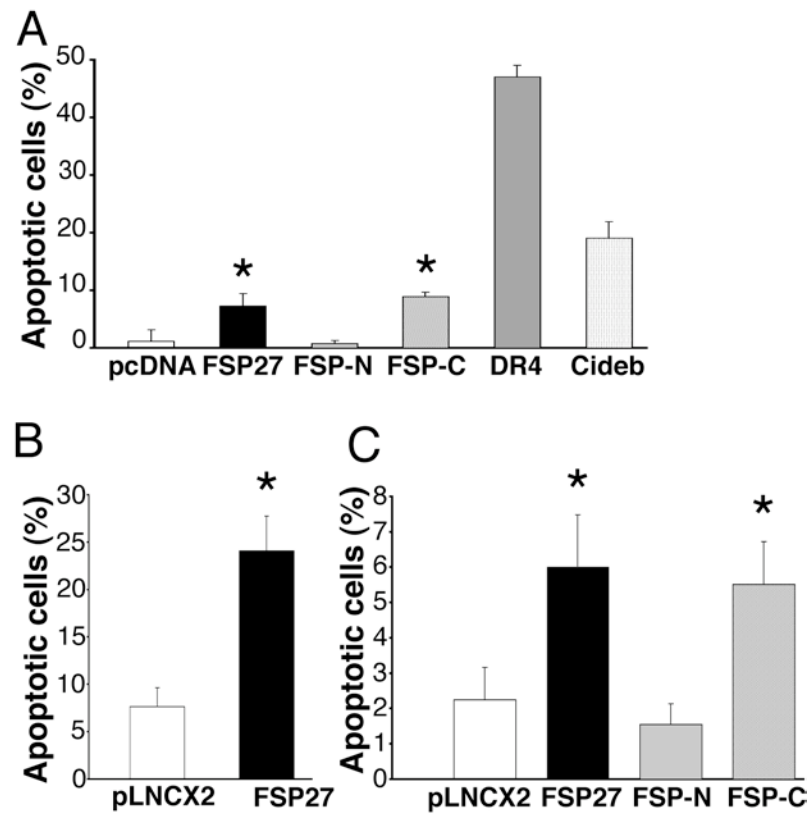


Figure 2

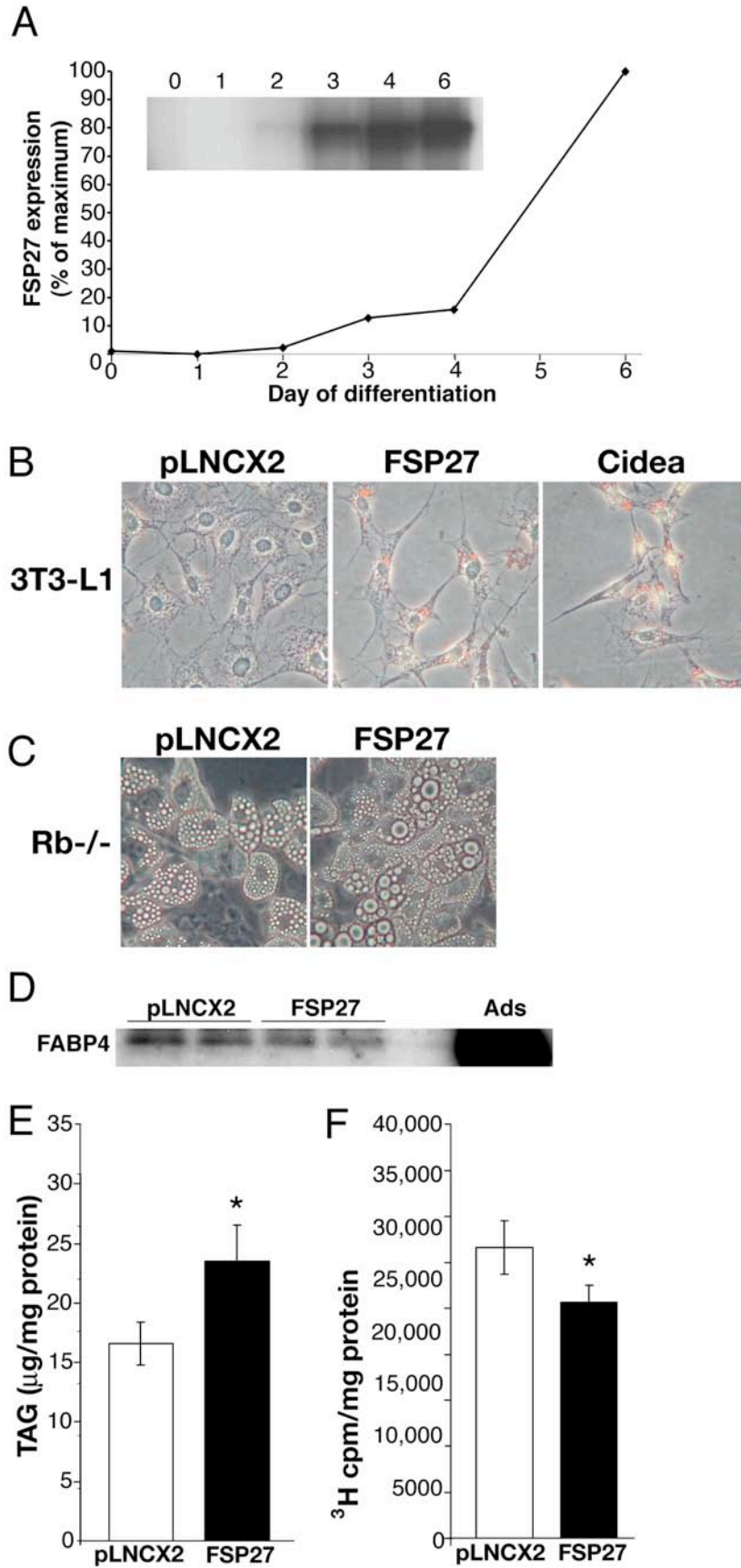


Figure 3

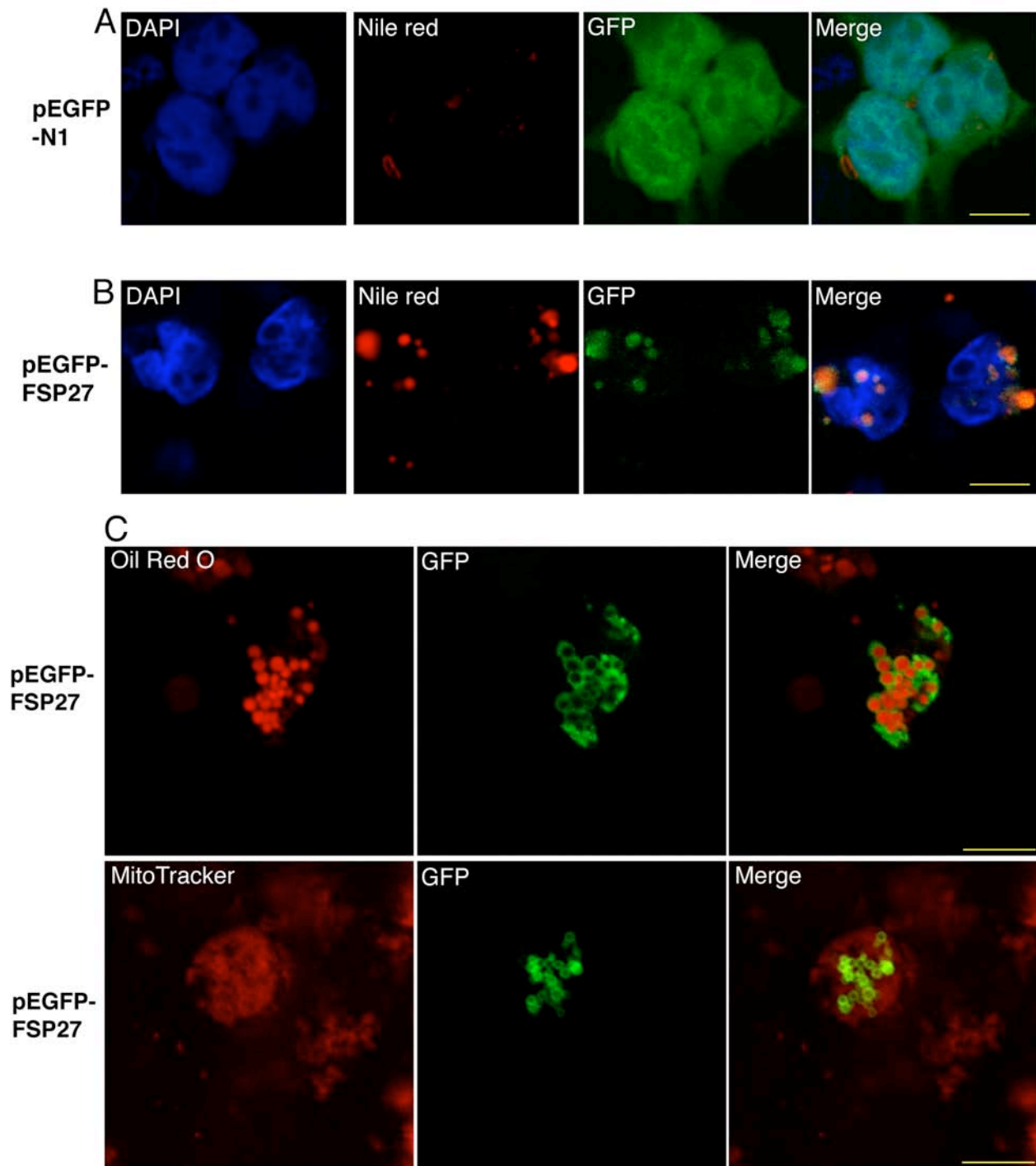


Figure 4

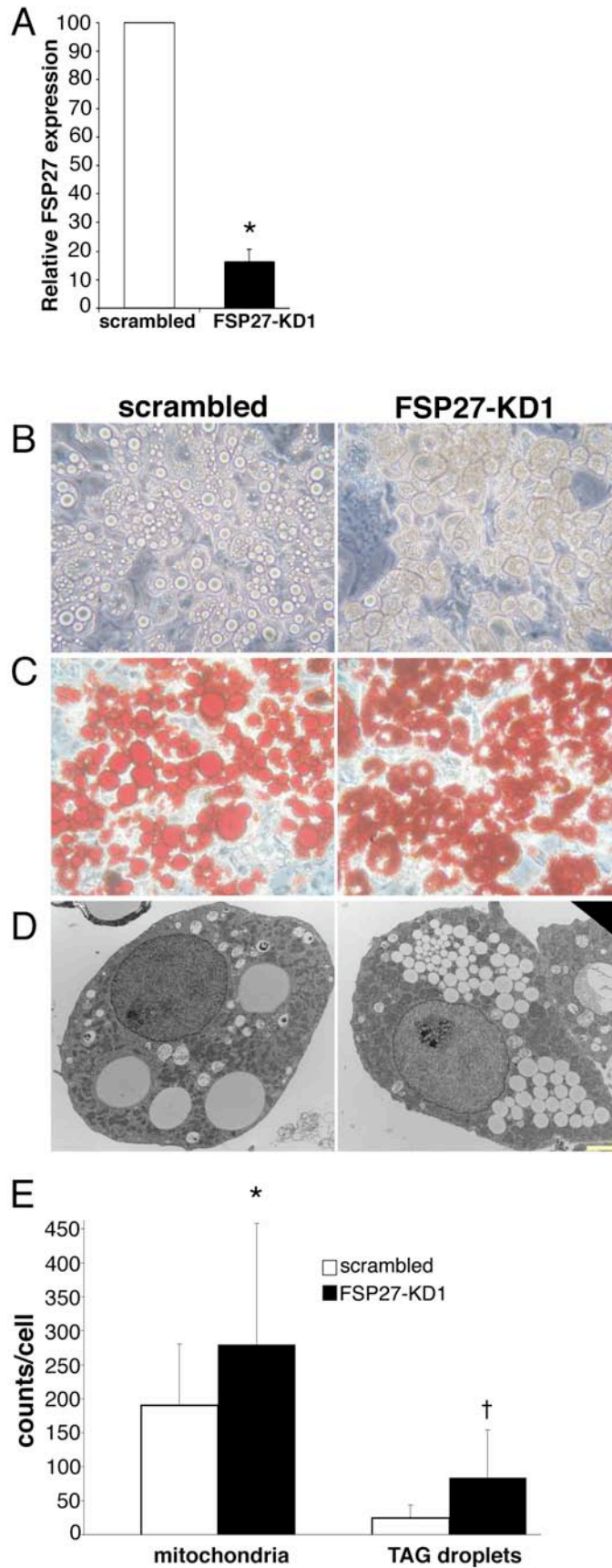


Figure 5

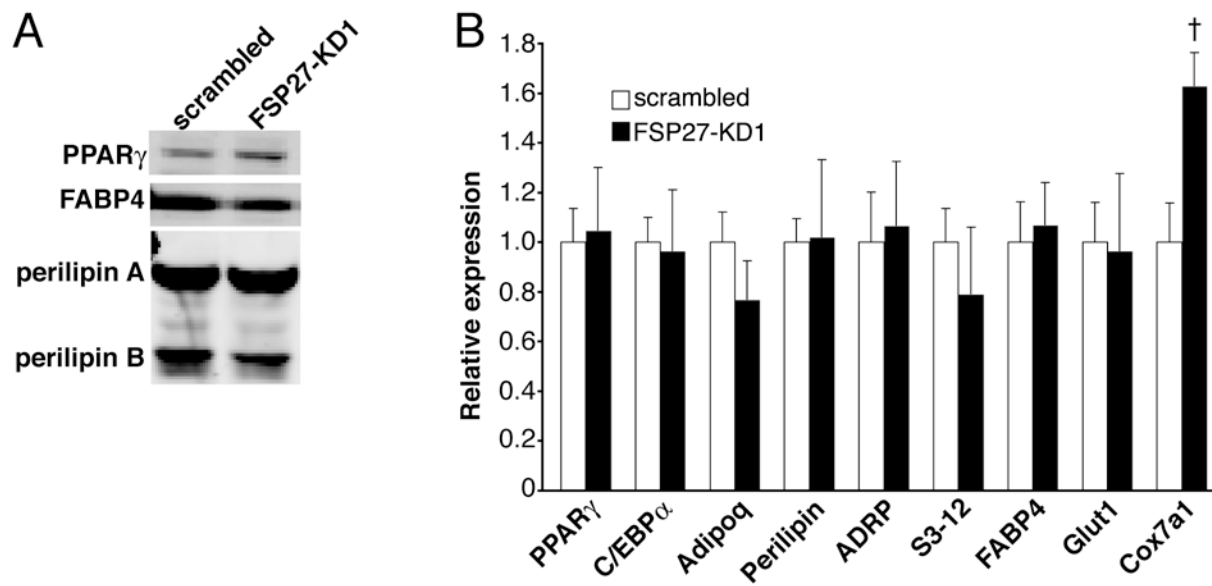


Figure 6

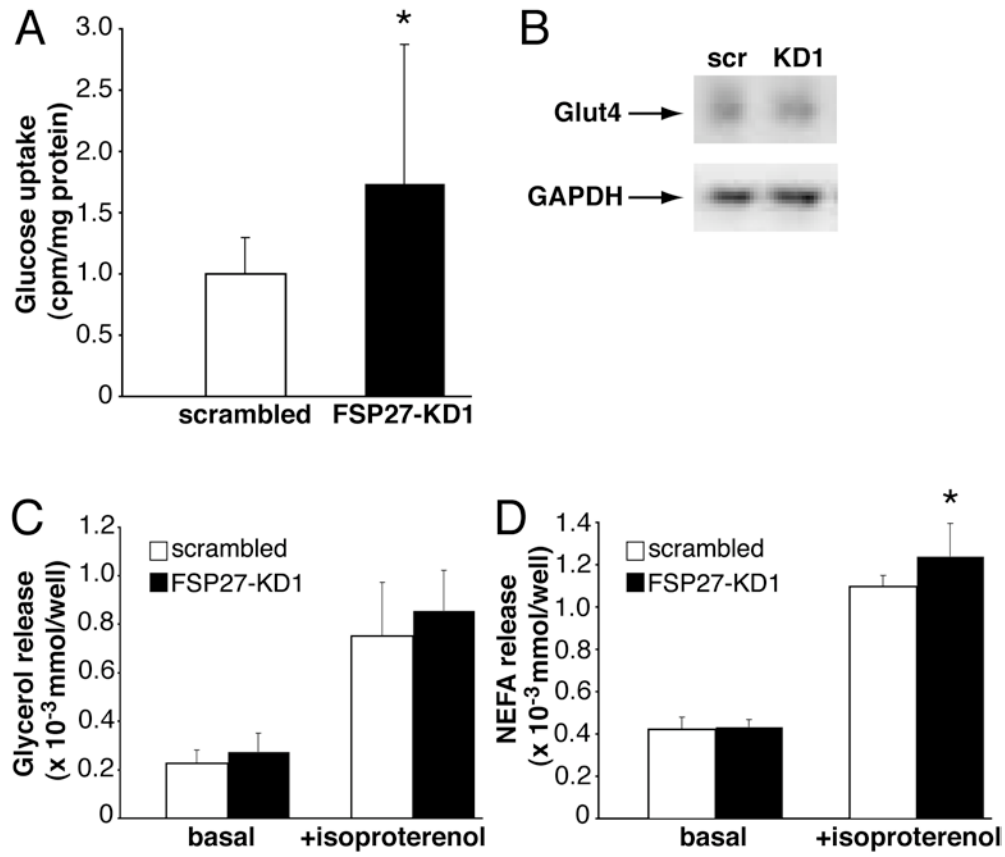
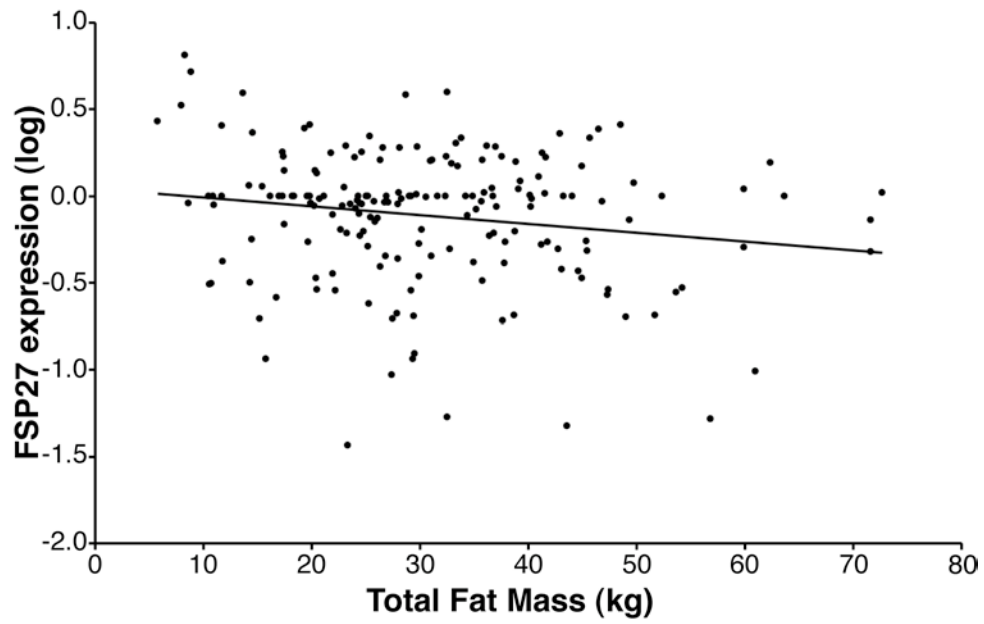


Figure 7



**Table 1.** Expression of markers specific for white and brown adipose tissue harvested from cultured brown adipocytes, brown adipose tissue (BAT), and 3T3-L1 adipocytes expressing a scrambled shRNA or a shRNA targeting FSP27 (KD1). Data are presented as the mean Ct value ( $\pm$  S.D.) of three independent experiments performed in triplicate. Significant differences for three white adipocyte genes were observed between control and FSP27-deficient adipocytes as indicated (\*,  $p < 0.05$ ). Expression in brown adipocyte models is for comparison. ND = no data.

Gene expression (Ct levels)	Brown adipocytes	BAT	Scrambled	FSP27-KD1
Aldha1	20.59	25.45	24.57 (0.47)	24.97 (0.44)
Cidea	23.31	18.67	28.56 (1.64)	27.95 (0.65)
Meox2	22.41	24.63	38.87 (5.79)	35.24 (0.75)
Prdm16	25.82	26.46	ND	36.49 (0.69)
Tbx15	26.33	30.86	27.99 (0.15)	28.15 (0.17)
UCP-1	28.82	18.01	35.03 (0.57)	34.46 (0.52)
Zic1	23.36	25.68	33.64 (2.05)	33.12 (1.84)
IGFBP3	20.92	25.24	27.14 (0.40)	26.18 (0.28)*
Dpt	20.86	23.59	21.24 (0.12)	22.11 (0.28)*
Wnt4	28.78	32.07	27.24 (0.57)	28.51 (0.66)*